Applied Physics Letters

# Design of flexible piezoelectric gyroscope for structural health monitoring

Cite as: Appl. Phys. Lett. **115**, 241901 (2019); https://doi.org/10.1063/1.5126409
Submitted: 02 September 2019 . Accepted: 23 November 2019 . Published Online: 09 December 2019

Yunqi Cao, and Nelson Sepúlveda



Applied Physics Letters ARTICLE scitation.org/journal/apl

# Design of flexible piezoelectric gyroscope for structural health monitoring

Cite as: Appl. Phys. Lett. **115**, 241901 (2019); doi: 10.1063/1.5126409
Submitted: 2 September 2019 · Accepted: 23 November 2019 ·
Published Online: 9 December 2019



Yunqi Cao and Nelson Sepúlveda[a)]

## AFFILIATIONS

Department of Electrical and Computer Engineering, Michigan State University, East Lansing, Michigan 48824, USA

[a)]Electronic mail: nelsons@egr.msu.edu

## ABSTRACT

This Letter reports a piezoelectric bending sensor configuration based on a complementary design of four identical flexible piezoelectric sensors using both theoretical analysis and experimental demonstration. The active material used here for sensing is a flexible ferroelectret polymer, which possesses a cellular internal structure with distributed trapped charges. The transverse piezoelectric effect is observed by changing the permanent macroscaled dipole moments upon bending. It has been found that the voltage output for the sensor is linearly related to the bending curvature. Angular displacement is determined by monitoring the output of four orthogonal devices on a rod. Different types of surface stress can also be determined by measuring output polarities from an antiparallel electrical connection. The proposed sensor configuration in this work is capable of providing a nondestructive evaluation of structural health by measuring a 2D bending vector.



As underground electric power transmission and water/gas pipes become more common, it is essential to develop technologies that can monitor their structural health. Landslides, seismic waves, or even nearby constructions could damage underground lines and cause severe damage. Nondestructive evaluation of structural health[1,2] becomes inevitable for long-term monitoring of structural distortion. Perhaps the most straightforward method for measuring structure deformation is to use a strain gauge as a transducer. Based on different working principles, such devices can be categorized into following groups: optical,[3] acoustic,[4] resistive,[5] and piezoelectric types.[6,7] Resistive strain gauges are most widely used due to their low fabrication costs and easy evaluation methods. However, those passive devices require extra costs in power consumption and maintenance. Piezoelectric materials have demonstrated potential applications in structural health monitoring[8–10] and bending curvature sensing[11,12] due to their high sensitivity and flexibility. Fully battery-less sensing networks can also be achieved by integrating piezoelectric sensors into an energy harnessing system.[13] However, little effort has been made to provide a design rule for 2D directional bending mapping especially by using the polarity of piezoelectric materials.

In previous work,[14] we developed the theoretical framework of the transverse piezoelectric effect of polypropylene ferroelectret (PPFE) and demonstrated its performance in terms of mechanical robustness, thermal stability, and humidity resistance. This manuscript focuses on a specific configuration of piezoelectric based bending gauge for structural health monitoring. Each of the four sensors is made of an 80 $\mu$m thick, 50 mm long, and 15 mm wide PPFE film, which has a $d_{31}$ value of approximately 2 pC/N,[15] sandwiched between two 500 nm thick sputtered silver metal electrodes. Figure 1 shows the SEM image of the cross-sectional view of the PPFE film. The piezoelectric effect of the PPFE film is introduced into the material by the following method. First, a solid polypropylene film filled with silicate particles (stress concentrates) is under a bidirectional in-plane stretching process to create microcracks. Then, high pressure (~5 MPa) $N_2$ gas is introduced and diffuses into the material to further expand the voids into ellipsoid shapes. A large electric field is applied and the discharging of plasma occurs in the voids, which induces trapped charges $q_i$ on top and bottom surfaces of the voids with opposite polarities. Therefore, each charged microvoid can be considered as a macrodipole moment $p_i = q_i l_i$, and the total displacement field can be expressed as $P = \Sigma_{i=1}^{N} p_i / V$, where $l_i$ is the separation of the top and bottom surfaces of a void, $N$ is the total voids in the materials, and $V$ denotes the volume of material. When an external mechanical load is applied, the distortions in $l_i$ result in a change in $P$, which leads to an electric output.

The sensor configuration is schematically shown in Figs. 2(a) and 2(b), where four sensors (sensors 1–4) are mounted on the outer surface of a Polyvinyl Chloride (PVC) pipe. Each sensor pair (sensor-1/2 and sensor-3/4) is connected in the antiparallel direction and aligned 180° with respect to the $z$- and $y$-axes, respectively. In this symmetric

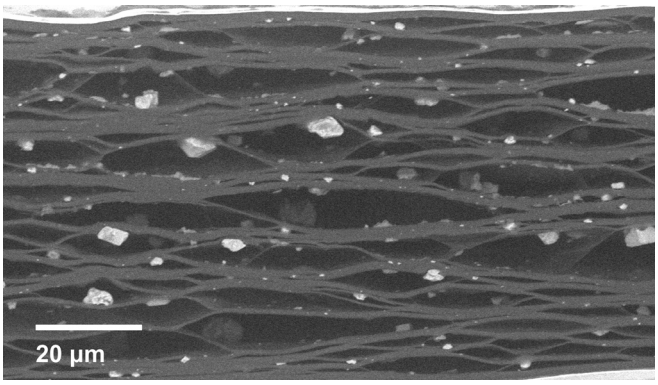


**FIG. 1.** SEM image of the cross-sectional view of the PPFE film. Particles shown are inorganic silicates.

design, the terminals $V_z$ and $V_y$ correspond to the electric output from sensor-1/2 and sensor-3/4, respectively, and monitor the structural deflection in that specific direction. During the experiments, the deflection of the pipe is provided by conducting a four-point bending test, where the two ends of the pipeline are fixed, and the two loading points are periodically driven by a computer-aided stepping motor through the pulse width modulation (PWM) method. Figures 2(c)–2(e) show the Finite Element Method (FEM) analysis for the experiments. When the pipe undergoes a lateral deflection $A(x)$ (either in the "$z$" or "$y$" direction), the structure deforms into a sinusoidal shape. Given a pipe length $L$, the deflected profile in the "$z$" or "$y$" directions along the pipe's length ($x$-axis) can be described as $A(x) = A_0[1 + \cos(2\pi x/L)]/2$,[14] where the origin is chosen to be the (0,0) coordinates of the $zy$-plane (i.e., center of the pipe) and $A_0$ denotes the maximum deflection. Since this $A_0$ is directly provided by the linear displacement of the stepping motor, $A_0$ exhibits a periodic triangular profile with respect to time. Figure 2(d) shows the FEM result of the buckling profile by applying different $A_0$ values at the origin from 0 to 1 cm. Assuming that $A(x)$ represents the displacement in the $z$-axis, the strain in the center of the pipe can be described as $\epsilon_x = z/\rho, -r < z < r$,[16] where $\rho$ is the radius of curvature at the center [see Fig. 2(d)] and $r$ is the outer radius of the pipe [see Fig. 2(a)]. Thus, the maximum strain occurs on the outer surface of the pipe and can be expressed as $\epsilon_{\max} = \pm r/\rho$, where the plus and minus notations represent the tensile and compressive stress, respectively. Given that the bending curvature ($\kappa$) is the reciprocal of the radius of curvature ($\rho$), it follows that $1/\rho = \kappa = |A''(0)|$, where $A''(0)$ is the second derivative of $A(x = 0)$ with respect to $x$ and $\epsilon_{max}$ is linearly proportional to $\kappa$. $\epsilon_{max}$ can be expressed in terms of the deflection by the following equation:

$$\epsilon_{\max} = \pm \frac{2\pi^2 r}{L^2} A_0. \tag{1}$$

From Eq. (1), it can be seen that $\epsilon_{max}$, which occurs at the center of the pipe, is proportional to the deflection amplitude at that location. This result is also consistent with the FEM result shown in Fig. 2(e), where $\epsilon_{max}$ is the stress plateau in the center area of the pipe, while the deflection increases linearly with the mechanical input $A_0$ as shown in Fig. 2(d). When a PPFE sensor is attached to the outer surface of the pipe and subjected to a bending moment, the longitudinal strain ($\epsilon_x$) in the film would induce a transverse piezoelectric effect[14] in the poling direction of the material, which is perpendicular to the film surface. In this case, the displacement field $D_n$ can be expressed as $D_n = \bar{k}E_n - \bar{d}\epsilon_x$, where $\bar{k}$ is the effective spring constant of PPFE, $E_n$ is the electric field, and $\bar{d}$ is the effective piezoelectric coefficient. Thus, the open circuit voltage $V_{oc}$ can be determined as $V_{oc} = h\epsilon_x\bar{d}/\bar{k}$,[14] where $h$ is the thickness of the PPFE film. Combining this expression for $V_{oc}$ with Eq. (1), the relation between $V_{oc}$, $A_0$, and $\kappa$ can be described as

$$V_{oc} = \pm \frac{2\pi^2 \bar{d} r h}{\bar{k} L^2} A_0 = \pm \frac{hr\bar{d}}{\bar{k}} \kappa. \tag{2}$$

Equation (2) shows that the magnitude of $V_{oc}$ is linearly proportional to both $A_0$ and $\kappa$, and its polarity is determined by the type of stress, i.e., whether it is tensile or compressive stress.

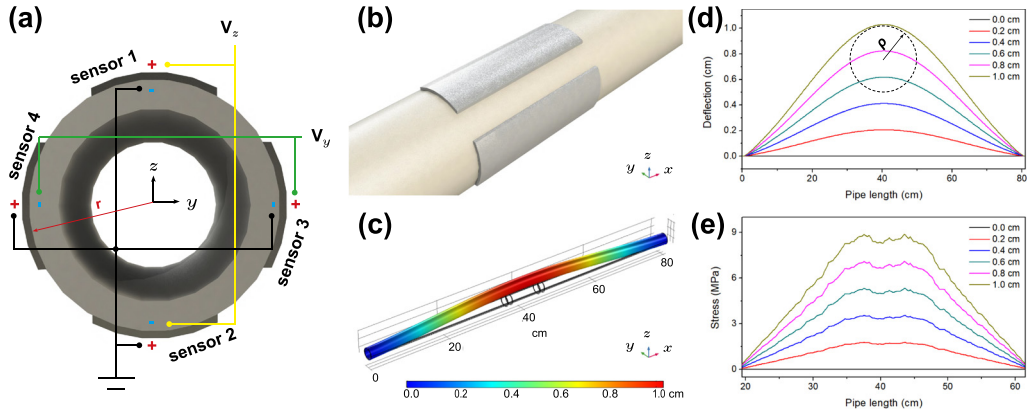


**FIG. 2.** Demonstration of a PVC pipe under the four-point bending test. (a) The schematic cross-sectional view of four PPFE bending sensors mounted on the PVC pipe with connections of different polarities. (b) A schematic side view of (a), where PPFE sensors are mounted on the surface of the PVC pipe. (c) FEM simulation of the PVC pipe under the four-point bending test. (d) FEM simulation results of deflection profiles under different lateral displacements. (e) FEM simulation results of surface stress distribution along the beam length under different lateral displacements described in (d).

Figures 3(a)–3(d) show the characterization of a single sensor under both tensile stress and compressive stress. It can be seen from Fig. 3(a) that when the sensor is attached on the tensile side of a bending pipe, $V_{oc}$ shows a positive value, while a negative value is observed on the compressive side [see Fig. 3(b)]. It should be noted that when measuring the open circuit voltage, an instrument with higher internal impedance must be used. A low impedance voltmeter would lead to a second-order system and the output voltage will be dependent on bending dynamics, which results in alternative positive and negative peaks.[17] Thus, a voltmeter with an input impedance of >1 GΩ (NI-9222, National Instruments) is used here, and the impedance of PPFE is estimated to be around 600 MΩ by characterizing the maximum power transfer.[18] In this case, the voltage measurements shown in Fig. 3 present unidirectional output signals, which are exactly the linear coupling effect between mechanical and electrical domains for piezoelectric materials. These results are also in agreement with Eq. (2) and demonstrate that the PPFE can be used for sensing not only the bending curvature but also the stress type.

It is also verified experimentally that changing polarity produces the same $V_{oc}$ magnitudes [see Figs. 3(a)–3(d)]. Thus, the combination of four identical sensors in a specific way as shown in Fig. 2(a) can be used to monitor the bending curvature with 2D directional information. For instance, when $A_0$ travels along the + $z$-axis, $V_z$ measures the electric output from sensors 1 and 2. Figure 3(e) shows the $V_{oc}$ measurement as a function of bending curvature, where a linear relation is observed as expected from Eq. (2). It should be noted that since PPFE operates as a current source, connecting sensors 1 and 2 in the antiparallel configuration results in current flowing in the same direction when the two sensors are experiencing different types of stresses (i.e., sensor 1 undergoes tensile stress, while sensor 2 undergoes compressive stress when $A_0$ travels in the + $z$ direction). Therefore, the voltage output is the same as using just one sensor but not expected to be doubled as shown in previous works.[17,18] However, sensors 3 and 4 are connected in the antiparallel direction but under the same types of stress for a + $z$ directional bending, which leads to the current flowing in opposite directions, and thus, $V_y = 0$, as shown in Fig. 3(f). Therefore, the advantage of using this 4-sensor configuration can be seen by comparing with the 2-sensor configuration (single sensor in $z$- and $y$-axes) as shown in Fig. 3(f), where the 2-sensor configuration incorrectly indicates a bending curvature in the $y$-axis under a pure bending in the $z$-axis.

When the pipeline is under an arbitrary deflection, the bending curvature can be described by the vector decomposition in a polar coordinate system. In the following, it is assumed that sensors 1 and 2 and sensors 3 and 4 are aligned in $z$- and $y$-axes, respectively [as shown in Fig. 2(a)] and the normal direction of a deflection is at the angle of $\theta$ to the $z$-axis. Then, $V_z$ and $V_y$ can be expressed as $V_z = V_z(0)\cos(\theta)$ and $V_y = V_z(0)\sin(\theta)$, where $V_z(0)$ is the open circuit voltage of $V_z$ at $\theta = 0$. Figure 4(a) shows $|V_z|$ of sensors 1 and 2 under various bending curvatures and directions $\kappa(\theta)$. It can be seen that $|V_z|$ starts with its maximum value at $\theta = 0$ and decreases as the bending normal direction approaches parallel to the $y$-axis. The relation between $|V_y|$ and $\kappa(\theta)$ demonstrated by sensors 3 and 4 is shown in Fig. 4(b), where the similar behavior along the $y$-axis confirms the symmetric property of the sensor pair configuration. It should be noted that using only sensors 1 and 2 or sensors 3 and 4 does not provide a full picture of real bending input. At a given measured $V_z$ or $V_y$ value, it is not enough to determine if the bending is under a normal directional bending along the $z$-($y$-) axis, or it is under a larger bending with an angle $\theta$ to the $z$-($y$-) axis. Thus, information from both sensor pairs (i.e., 1 and 2 and 3 and 4) needs to be collected for a full description of the bending. According to Eq. (2), the bending curvature and direction can be determined as

$$\kappa(\theta) = \frac{\bar{k}}{h\bar{d}r} V_\theta, \tag{3}$$

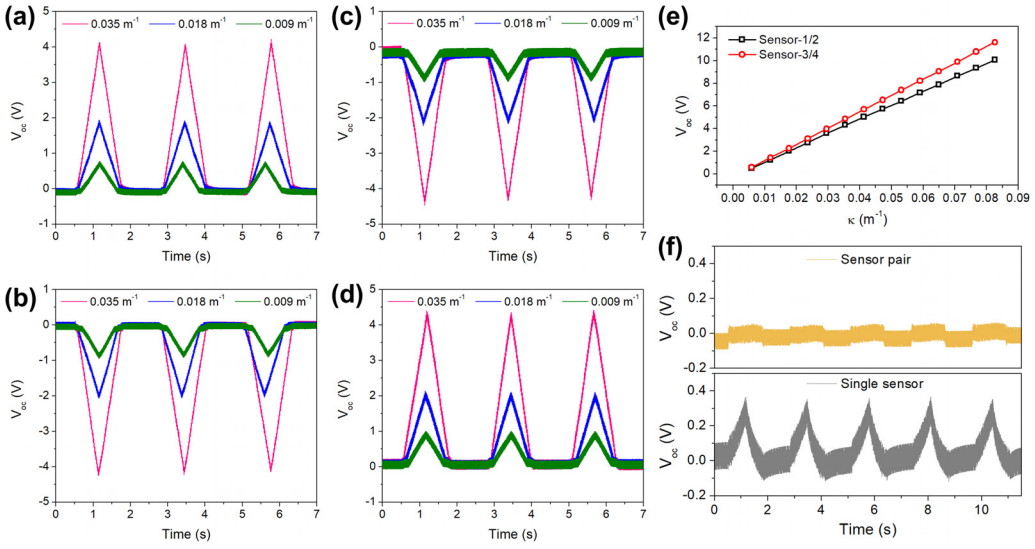


**FIG. 3.** Characterization of the PPFE sensor and sensor pair under different bending curvatures. (a) Single PPFE sensor on the tensile side with a positive connection. (b) Single PPFE sensor on the compressive side with a positive connection. (c) Single PPFE sensor on the tensile side with a negative connection. (d) Single PPFE sensor on the compressive side with a negative connection. (e) $V_{oc}$ of sensor pairs under different bending curvatures. (f) Demonstration of cancelation by using the sensor pair.

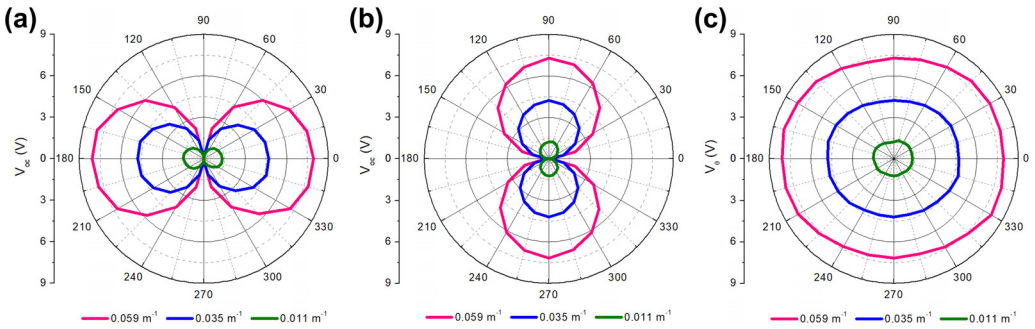


**FIG. 4.** Polar plots of $V_{oc}$ under different bending curvatures in arbitrary directions. (a) $V_{oc}$ of Sensors 1 and 2 under different bending curvatures. (b) $V_{oc}$ of Sensors 3 and 4 under different bending curvatures. (c) Polar plots of $V_\theta$ calculated from $V_{oc}$ of Sensors 1 and 2 and Sensors 3 and 4, which describe the structural deformation in arbitrary directions.

and

$$\theta = arctan\frac{V_y}{V_z}, \tag{4}$$

where $V_\theta = \sqrt{V_y^2 + V_z^2}$. Figure 4(c) shows the 2D plot of the relation between $V_\theta$ and $\kappa(\theta)$. Each circle plot represents a bending condition under a specific $\kappa$ value, which can be related to $V_\theta$ through Eq. (3). The directional information $\theta$ is also able to be determined through Eq. (4). Hence, in order to obtain the detailed bending information of a buried and obscured pipeline, only two parameters, $V_z$ and $V_y$, are required, while four measurements are required when using the traditional resistive bending gauge for the same purpose. It is also worth mentioning that this design utilizes the polarities of piezoelectric and ferroelectric materials when subjected to different types of stresses and different electrical connections. Therefore, the choice of materials is not restricted to PPFE.

In this work, a specific configuration of monitoring the structural health is proposed based on piezoelectric bending sensors. Four identical PPFE films are patterned on the outer surface of the structure under test. Each of the two sensor pairs is connected in the antiparallel direction and aligned in the perpendicular direction with the other. Based on the transverse piezoelectric effect of PPFE and the inherent polarity characteristic of piezoelectric materials, the designed sensing network is able to provide a 2D full description of an arbitrary deformation. Two open circuit voltages are used to measure different bending conditions, where $V_\theta$ is found to be linearly related to the bending curvature and the directional information $\theta$ can also be determined.

This work was supported in part by the National Science Foundation (NSF ECCS Award No. ECCS:1854750) and by the MSU Strategic Partnership Grant (No. 16-SPG-Full-3236). The authors would also like to thank the Center for Advanced Microscopy (CAM) at Michigan State University.

## REFERENCES

[1]P. C. Chang, A. Flatau, and S. Liu, Struct. Health Monit. **2**, 257 (2003).
[2]J. Ko and Y. Ni, Eng. Struct. **27**, 1715 (2005).
[3]M. D. Todd, J. M. Nichols, S. T. Trickey, M. Seaver, C. J. Nichols, and L. N. Virgin, Philos. Trans. R. Soc., A **365**, 317 (2006).
[4]A. Behnia, H. K. Chai, and T. Shiotani, Constr. Build. Mater. **65**, 282 (2014).
[5]Y. Kim, Y. Kim, C. Lee, and S. Kwon, IEEE Sens. J. **10**, 1320 (2010).
[6]W. Staszewski, G. Tomlinson, C. Boller, and G. Tomlinson, *Health Monitoring of Aerospace Structures* (Wiley Online Library, 2004).
[7]M. Lin, X. Qing, A. Kumar, and S. J. Beard, Proc. SPIE **4332**, 98–107 (2001).
[8]G. Park, H. Sohn, C. R. Farrar, and D. J. Inman, Shock Vib. Dig. **35**, 451 (2003).
[9]S. Guo, S. Chen, L. Zhang, W. H. Liew, and K. Yao, NDT&E Int. **107**, 102131 (2019).
[10]W. Na and J. Baek, Sensors **18**, 1307 (2018).
[11]Z. Liu, Z. Zhao, X. Zeng, X. Fu, and Y. Hu, J. Phys. D: Appl. Phys. **52**, 314002 (2019).
[12]Y. Xin, T. Liu, H. Sun, Y. Xu, J. Zhu, C. Qian, and T. Lin, Ferroelectrics **531**, 102 (2018).
[13]S. C. Lai, K. Yao, and C. Y. Tan, IEEE Sens. J. **16**, 7841 (2016).
[14]Y. Cao, W. Li, and N. Sepúveda, IEEE Sens. J. **19**, 10327 (2019).
[15]G. Neugschwandtner, R. Schwödiauer, M. Vieytes, S. Bauer-Gogonea, S. Bauer, J. Hillenbrand, R. Kressmann, G. Sessler, M. Paajanen, and J. Lekkala, Appl. Phys. Lett. **77**, 3827 (2000).
[16]T. G. Byrom, *Casing and Liners for Drilling and Completion* (Elsevier, 2013).
[17]Y. Cao, J. Figueroa, W. Li, Z. Chen, Z. L. Wang, and N. Sepúlveda, Nano Energy **63**, 103852 (2019).
[18]Y. Cao, J. Figueroa, J. Pastrana, W. Li, Z. Chen, Z. Wang, and N. Sepulveda, ACS Appl. Mater. Interfaces **11**, 17400 (2019).